Cell Stem Cell
Article

Selective Elimination of Human Pluripotent Stem Cells by an Oleate Synthesis Inhibitor Discovered in a High-Throughput Screen

Uri Ben-David,[1,2] Qing-Fen Gan,[3] Tamar Golan-Lev,[1,2] Payal Arora,[3] Ofra Yanuka,[1,2] Yifat S. Oren,[2] Alicia Leikin-Frenkel,[4,5] Martin Graf,[6] Ralph Garippa,[3,7] Markus Boehringer,[6] Gianni Gromo,[6] and Nissim Benvenisty[1,2,*]
[1]Stem Cell Unit
[2]Department of Genetics, Silberman Institute of Life Sciences
The Hebrew University, Jerusalem 91904, Israel
[3]Hoffmann-La Roche, Nutley, NJ 07110, USA
[4]The Bert W. Strassburger Lipid Center, Sheba Medical Center, Tel Hashomer 52621, Israel
[5]Sackler School of Medicine, Tel Aviv University, Tel Aviv 69978, Israel
[6]F. Hoffmann-La Roche AG, Basel 4070, Switzerland
[7]Present address: Memorial Sloan-Kettering Cancer Center, New York, NY 10065, USA
*Correspondence: nissimb@cc.huji.ac.il
http://dx.doi.org/10.1016/j.stem.2012.11.015

SUMMARY

The use of human pluripotent stem cells (hPSCs) in cell therapy is hindered by the tumorigenic risk from residual undifferentiated cells. Here we performed a high-throughput screen of over 52,000 small molecules and identified 15 pluripotent cell-specific inhibitors (PluriSIns), nine of which share a common structural moiety. The PluriSIns selectively eliminated hPSCs while sparing a large array of progenitor and differentiated cells. Cellular and molecular analyses demonstrated that the most selective compound, PluriSIn #1, induces ER stress, protein synthesis attenuation, and apoptosis in hPSCs. Close examination identified this molecule as an inhibitor of stearoyl-coA desaturase (SCD1), the key enzyme in oleic acid biosynthesis, revealing a unique role for lipid metabolism in hPSCs. PluriSIn #1 was also cytotoxic to mouse blastocysts, indicating that the dependence on oleate is inherent to the pluripotent state. Finally, application of PluriSIn #1 prevented teratoma formation from tumorigenic undifferentiated cells. These findings should increase the safety of hPSC-based treatments.

INTRODUCTION

Human pluripotent stem cells (hPSCs) hold great promise for regenerative medicine due to their unique abilities to self-renew and to differentiate into all the cell types of the human body. However, the same properties also make these cells tumorigenic, and therefore tumor formation was found to positively correlate with the residual presence of undifferentiated pluripotent cells (Miura et al., 2009). As very few hPSCs are sufficient for teratoma formation (Hentze et al., 2009; Lee et al., 2009), it is essential to eliminate residual pluripotent cells prior to the clinical application of their derivatives (Ben-David and Benvenisty, 2011). Importantly, while the generation of induced pluripotent stem cells (iPSCs) may have resolved the problem of immunogenic rejection, the risk of teratoma formation remains a major obstacle that is equally relevant for embryonic stem cells (ESCs) and for iPSCs (Ben-David and Benvenisty, 2011; Miura et al., 2009).

To promote the removal of residual pluripotent cells from differentiated cultures, several strategies have been suggested, including introduction of suicide genes (Schuldiner et al., 2003), interference with tumor progression genes (Blum et al., 2009) or with tumor suppressors (Menendez et al., 2012), cell sorting based on antibodies against PSC-specific surface antigens (Tang et al., 2011), and the use of cytotoxic antibodies (Choo et al., 2008). However, these methods are largely based either on genetic manipulations or on cell sorting, which are not optimal for cell therapy purposes. Furthermore, no single antibody or cycle of cell sorting completely removes undifferentiated cells from mixed cultures. Thus, current clinical trials largely depend on differentiation of human ESCs, using compounds that affect pathways such as BMP or TGFβ, with the hope that these differentiation protocols will minimize the residual existence of undifferentiated cells. Many preclinical trials in animals, however, demonstrate that even after long-term differentiation protocols, residual undifferentiated cells may still form tumors (Germain et al., 2012; Roy et al., 2006; Wernig et al., 2004; Xie et al., 2007). A more robust method for the elimination of undifferentiated hPSCs from culture is therefore required.

In order to identify small molecules that selectively perturb vital pathways in hPSCs, and thus induce cell death only in these cells, we designed and performed an unbiased high-throughput screen of small molecules. The desired small molecules should eliminate efficiently and robustly undifferentiated hPSCs from culture, without affecting their differentiated derivatives. Application of these small molecules to cultures of differentiated cells prior to their transplantation into patients would therefore decrease, and possibly abolish, the risk of tumor formation due to residual undifferentiated cells. A major advantage of this approach is that it does not require genetic manipulations or

single-cell dissociation, so that genetically normal hPSCs can be induced to differentiate into complex structures, which need not be disassembled prior to their transplantation.

RESULTS

Assay Development for High-Throughput Screen

Prior to the primary screen, we developed and optimized a protocol that enables the culture of undifferentiated hPSCs in a 384-well format, the automatic application of small molecules to these cell plates, and the accurate assessment of cell viability after the exposure of the cells to the compounds. Human ESCs and iPSCs were grown on matrigel-coated plates without feeders, using a serum-free defined medium (mTeSR1) (Ludwig et al., 2006). The pluripotency of the cells under these conditions was confirmed by their normal morphology, their positive staining for alkaline phosphatase (AP), and their expression of OCT4 (see Figures S1A and S1B available online). Cells were then harvested and seeded in 384-well plates, at a density of 5,000 cells per well. The cells maintained their normal morphology, formed colonies, and proliferated. Quantitative PCR and immunofluorescence (IF) staining for OCT4 verified that the cells remained undifferentiated for at least 5 days under these conditions (Figures S1C and S1D). For the accurate measurement of the number of viable cells in culture, an ATP-based luminescent cell viability assay (CellTiter-Glo) was applied. We verified in our undifferentiated cells that this assay accurately determines the number of viable cells in culture (Figures S1E and S1F). We also performed a pilot screen with 50 known cytotoxic compounds (Table S1) and selected two compounds as controls for the primary screening: amsacrine hydrochloride, a DNA topoisomerase inhibitor, and cyclohexamide, a translation inhibitor (Figures S1G and S1H).

High-Throughput Screen Identifies Cytotoxic Inhibitors of hPSCs

In order to identify potent cytotoxic inhibitors of hPSCs, we screened 52,448 small molecules against undifferentiated human ESCs. These molecules constitute a representative subset of the Hoffmann-La Roche compound library, comprised of diverse chemical entities (see Supplemental Experimental Procedures). Diploid human ESCs, CSES2 cells, were grown on matrigel-coated plates with the defined medium mTeSR1, their pluripotency was verified, and they were plated in 384-well plates. Twenty-four hours after cell plating, cells were exposed to the compounds, so that each of the 52,448 compounds was added to one well, at a final concentration of 20 μM (with 0.5% DMSO). Twenty-four hours after compound addition, cell viability was measured in each well. A schematic flow chart of the primary screen is presented in Figure 1A, and representative plate results are presented in Figure 1B.

The primary screen was very robust, as determined by its high Z' factor (0.78 ± 0.06, Figure S1I). "Hits" were defined as compounds that induced over 60% reduction in the number of viable cells. Using this threshold, 2,031 compounds (<4% of the tested compounds) were selected (Figure 1C). As the primary screen was performed at a single concentration and without replicates, the first confirmation screen was performed to remove false positive hits. Screening replicates of two independently derived human ESC lines (CSES2 and H9) at a single concentration (20 μM) confirmed 696 hits that were cytotoxic for both cell lines (Figures 1D and 2B). Next, these 696 confirmed hits were tested against the human ESC line CSES2, and its clone CSES2-SO2/3, at eight concentrations (ranging from 50 μM to 23 nM, with 1:3 serial dilution steps). As expected, the cytotoxic effect of the compounds was dose dependent in >98% of the cases, and very high compound potency correlations were observed between all of the human ESCs tested (Figures 1D and 1E). To verify that the inhibitory effect of the compounds persists over time, we exposed CSES2 cells to six concentrations for 48 hr. The effect was maintained for all of these compounds, without any recovery observed (Figure S1J).

We then examined the effect of the compounds on human iPSCs. BJ-iPS28 cells were grown in the exact same conditions as the ESCs and were tested at six concentrations (ranging from 50 μM to 200 nM, with 1:3 serial dilution steps). The EC_{50} values (i.e., the effective concentrations that induce 50% reduction in cell number) obtained for the iPSCs were very similar to those of the ESCs, and no compounds were found to be cytotoxic toward one cell type without having a detrimental effect on the other (Figure 1F). Together, these data indicate that the identified compounds are indeed potent cytotoxic inhibitors of hPSCs.

Counter Screens Reveal Pluripotent-Specific Inhibitors

Next, we wanted to discover whether among the identified compounds some would be cytotoxic only toward hPSCs and not toward other cell types. We thus screened these 696 compounds against nine other cell types, representative of all germ layers and developmental stages (Figure 2A). Importantly, many of these cell types were differentiated from human ESCs or iPSCs. The screened cell types included ESC-derived neural stem cells (NSCs), ESC-derived mesenchymal stem cells (MSCs), ESC-derived endodermal progenitor cells, ESC-derived hepatocytes, iPSC-derived cardiomyocytes, fibroblasts from which the iPSC cell line BJ-iPS28 was derived, and three cancer cell lines: neuroblastoma (Kelly), cervical cancer (HeLa), and hepatocarcinoma (Huh7). Each cell type was screened in either a duplicate or a triplicate at 20 μM concentration. Encouragingly, the compound potency correlation between hPSCs and each of the other cell types was much weaker than that within hPSCs (Figures 2B and S2A–S2F). Unsupervised hierarchical clustering was performed using the compound inhibition profiles of all cell types. The result suggested that hPSCs indeed clustered together by their response to small molecules and revealed a subgroup of compounds highly cytotoxic specifically to these cells (Figure 2C).

In order to further verify the selective cytotoxicity of identified compounds, we screened them in multiple concentrations against differentiated cells that were genetically matched to the undifferentiated cells in our screen. CSES2-SO2/3 is a genetically labeled cell line that expresses mCherry under the promoter of the pluripotency hallmark gene *OCT4* and enhanced green fluorescent protein (EGFP) under the promoter of the early endodermal marker *SOX17* (Kopper and Benvenisty, 2012). Therefore, these cells are red while undifferentiated and become green when they differentiate into endodermal progenitors (Kopper and Benvenisty, 2012) (Figures S3A–S3C). Both the undifferentiated red cells and the differentiated green cells

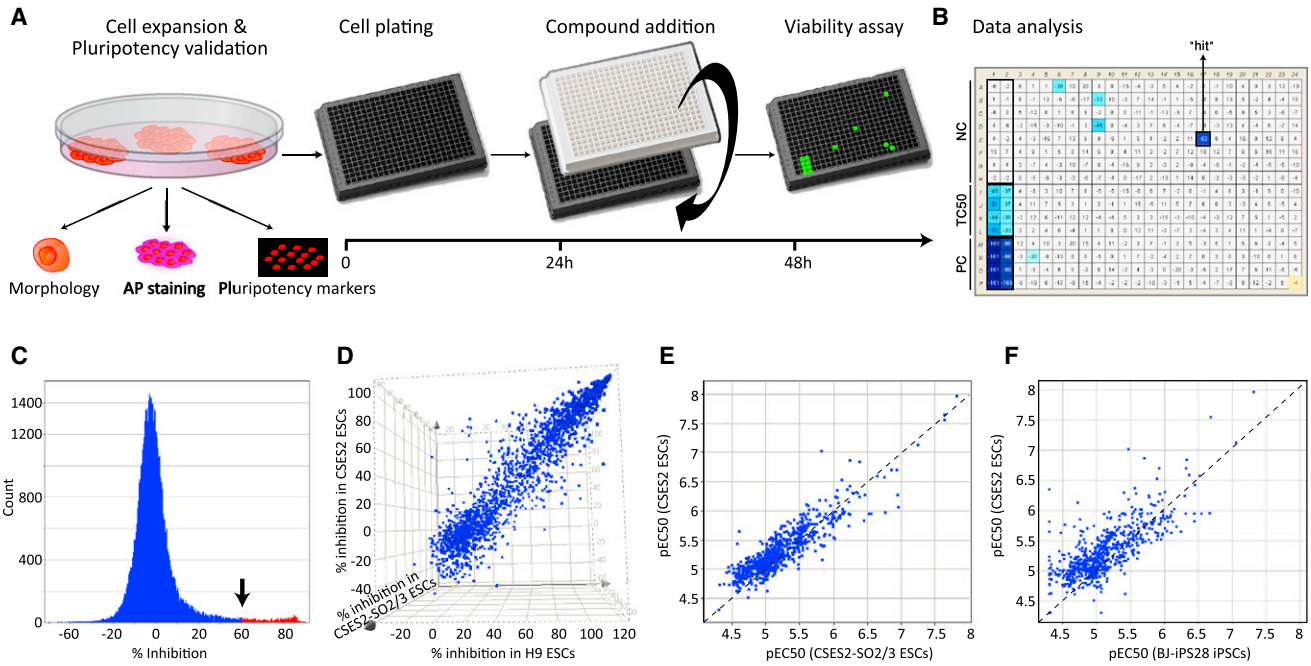

Figure 1. High-Throughput Screening of 52,448 Small Molecules against hPSCs

(A) A schematic representation of the primary screen flow chart.

(B) Representative results of one assay plate. NC, negative control, 0.5% DMSO; TC50, toxic compound that leads to ~50% cell death, cyclohexamide at 2 μM; PC, positive control, amsacrine hydrochloride at 5 μM. "Hits" were determined as compounds that induced over 60% reduction in the number of viable cells.

(C) A distribution plot of compound effect on cell viability. Arrow indicates the cutoff value; "hits" are marked in red.

(D) A three-dimensional scatterplot showing the response of three ESC lines to 2,031 compounds tested in a confirmation screen, at 20 μM concentration.

(E) A scatterplot comparing pEC_{50} values of 696 confirmed "hits" between two ESC lines: CSES2 and SO2/3. EC_{50} represents the half-maximal effective concentration value; $pEC_{50} = logEC_{50}$; correlation coefficient (r^2) = 0.80.

(F) A scatterplot comparing pEC_{50} values of 696 confirmed "hits" between ESC and iPSC lines (CSES2 and BJ-iPS28, respectively); correlation coefficient (r^2) = 0.57. See also Figure S1 and Table S1.

were screened at eight concentrations, so that reliable EC_{50} values could be calculated for these genetically identical cells (Figure 2D). Finally, we also screened at six concentrations the BJ fibroblasts from which the iPSC line BJ-iPS28 was derived and could thus generate reliable EC_{50} values for both the iPSCs and their somatic cells of origin (Figure 2D).

We set a very stringent threshold and identified compounds that induced above 80% inhibition in all of the hPSCs (at 20 μM) but less than 20% inhibition in other cell types (at the same high concentration). Moreover, we required the EC_{50} values to be around 5 μM or lower for CSES2, CSES2-SO2/3, and BJ-iPS28 but higher than 50 μM for the eight day-differentiated CSES2-SO2/3 cells and for the BJ fibroblasts. Fifteen compounds met or approached these stringent criteria (Figure 2E and Table S2), and we thus termed them pluripotent-specific inhibitors (PluriSIns). Human ESCs lose their sensitivity to PluriSIns upon their differentiation, whereas human somatic cells acquire this sensitivity upon their reprogramming to iPSCs (Figures 2F and S3D). Considering the short exposure duration used in our screen (24 hr) and the stringent threshold used for "hit" identification (>80% reduction in number of viable cells), we reasoned that the identified compounds could not be proliferation inhibitors but rather were cytotoxic compounds that actively eliminated hPSCs. In order to confirm the cytotoxic effect of PluriSIns in additional assays, cells were treated with PluriSIns and subjected to (1) ATP-independent methylene blue viability assay and (2) high-content microscopy imaging. Both independent assays confirmed the cytotoxicity of the PluriSIns toward hPSCs (Figures S4A and S4B).

In order to further verify the selectivity of the PluriSIns, we took advantage of the genetic labeling system described above. Undifferentiated and differentiated CSES2-SO2/3 cells were subjected to microscopy imaging after exposure to PluriSIns. This visualization verified the pluripotent-specific effect of PluriSIns, independently of the ATP-based viability assay, as the compounds clearly eliminated the red undifferentiated cells, without any detectable effect on the green differentiated cells (Figure 2G). Taken together, PluriSIns had a robust, rapid, and selective cytotoxic effect toward hPSCs.

PluriSIn #1 Mechanism of Action

Examination of the chemical structure of PluriSIns (Figure 3A) revealed that nine out of the 15 compounds share a common structural moiety, phenylhydrazine (Ph–N[H,C]–NH). This is an ~60-fold overrepresentation of this moiety compared to the entire screening library ($p < 10^{-16}$). Moreover, seven of these compounds share a more complex structure and can be defined as N-acyl phenylhydrazine derivatives (Ph– N[H,C]–NH–(C = C) n–[C,S] = [O,N], n = 0 or 1). This similarity may be linked to the mechanism of action or to the specificity of these PluriSIns.

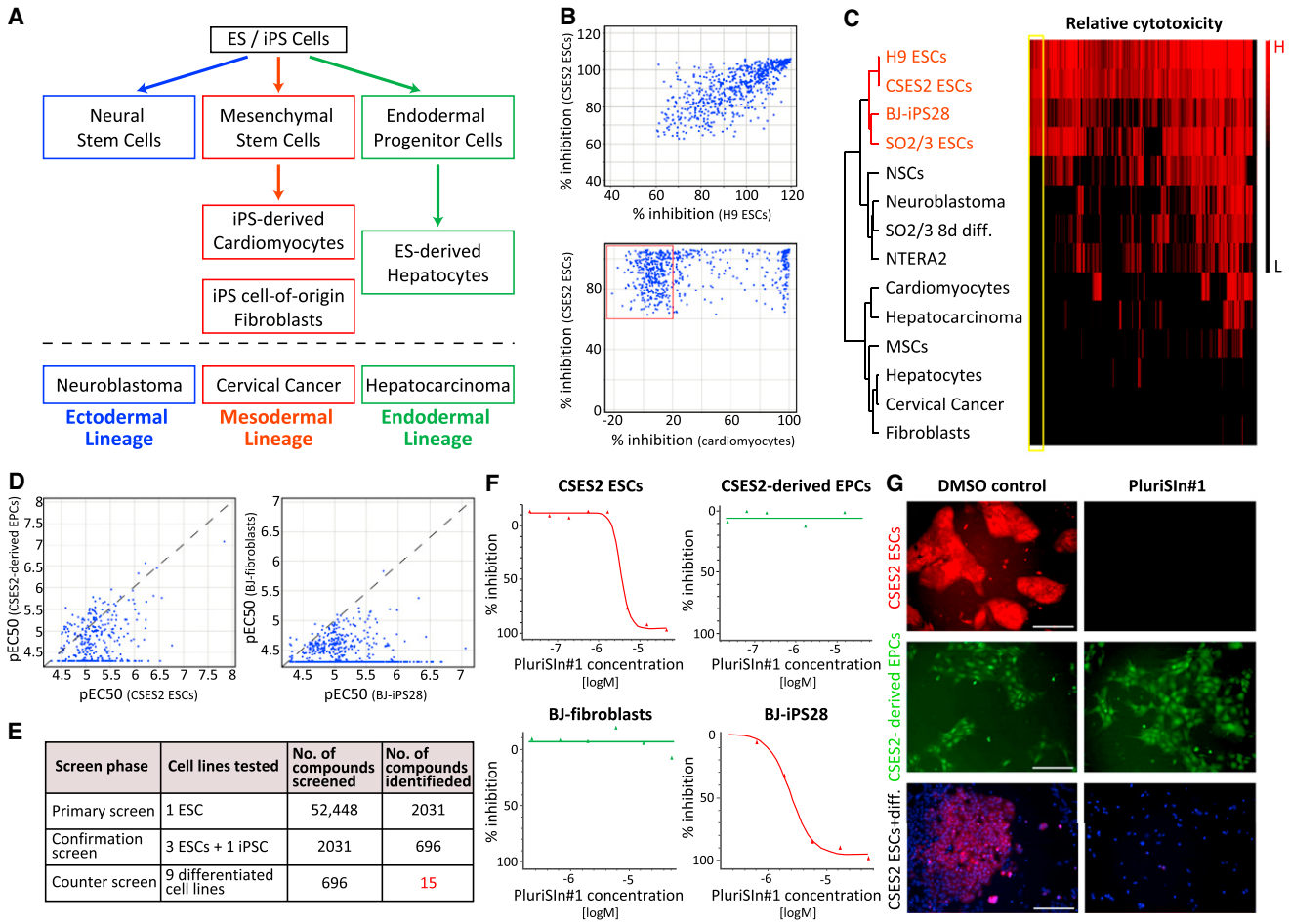

E

Screen phase	Cell lines tested	No. of compounds screened	No. of compounds identifieded
Primary screen	1 ESC	52,448	2031
Confirmation screen	3 ESCs + 1 iPSC	2031	696
Counter screen	9 differentiated cell lines	696	15

Figure 2. Identification of Pluripotent-Specific Inhibitors

(A) A schematic representation of the cell types used for the counter screen. Four PSCs and nine cell types of all germ layers and developmental stages were screened with the confirmed hPSC cytotoxic inhibitors from the primary screen.

(B) Scatterplots comparing the response to the 696 confirmed "hits" between the ESC line CSES2 and another ESC line (H9, top) or between CSES2 and iPSC-derived cardiomyocytes (bottom). Very high correlation exists between the pluripotent cells (r^2 = 0.87), whereas no correlation exists between the pluripotent and differentiated cells (r^2 = 0.03), demonstrating that many of the identified compounds are selectively cytotoxic toward human pluripotent stem cells (encircled in red).

(C) Unsupervised hierarchical clustering of all cell types based on their cytotoxic response to the confirmed "hits" at 20 μM concentration, showing that human pluripotent stem cells cluster together. Fifteen selective inhibitors of hPSCs (termed PluriSIns) were identified (yellow rectangle). Red and black represent high (100%) and low (0%) inhibition values, respectively.

(D) Scatterplots comparing pEC_{50} values of all confirmed "hits" between the human ESC line CSES2-SO2/3 and the endodermal progenitor cells (EPCs) differentiated from the same cell line (left; r^2 = 0.05) and between the human iPSC line BJ-iPS28 and the fibroblasts from which it was derived (right; r^2 < 0.01). Note that in both cases many compounds were found to be cytotoxic selectively toward the undifferentiated cells.

(E) A summary of the screen phases, the cell types used, the number of compounds tested, and the number of compounds identified in each phase.

(F) Representative dose response curves of PluriSIn #1, showing that ESCs lose their sensitivity to this compound after 8 days of differentiation (top), whereas somatic cells acquire such sensitivity upon their reprogramming to iPSCs (bottom).

(G) Fluorescence microscopy imaging, showing the differential response of undifferentiated cells (red), eight day-differentiated EPCs (green) and a mixed culture of undifferentiated and differentiated cells (nuclear staining in blue, undifferentiated cells in red) to PluriSIn #1 (at 20 μM). Scale bars represent 100 μm. See also Figures S2–S4 and Table S2.

In an attempt to identify their mechanism of action, we further explored the most potent and selective compound, PluriSIn #1 (also known as isonicotinic acid N'-phenyl-hydrazine), and another N-acyl phenylhydrazine derivative, PluriSIn #6. We applied a toxicogenomic approach to identify gene expression alterations after the exposure of the cells to the compounds. Unsupervised hierarchical clustering based on global gene expression profiling revealed marked gene expression changes in the PluriSIn-treated undifferentiated cells compared to their DMSO-treated controls, 12 hr after exposure to the compounds (Figure 3B).

Among the most deregulated genes, we detected several hallmark genes related to apoptosis (Figure 3C). Functional annotation analysis of deregulated genes (>2-fold change) was

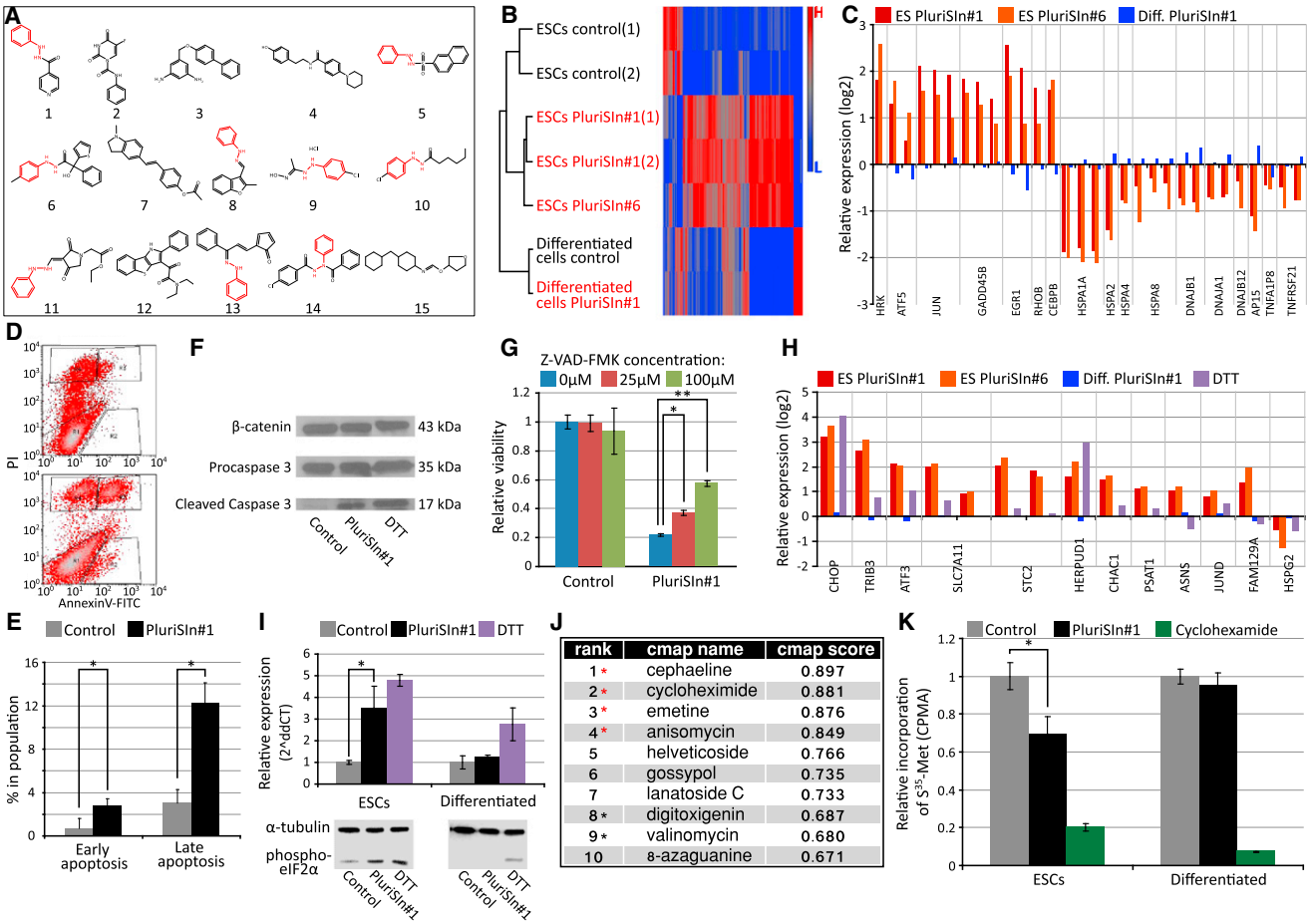

rank	cmap name	cmap score
1*	cephaeline	0.897
2*	cycloheximide	0.881
3*	emetine	0.876
4*	anisomycin	0.849
5	helveticoside	0.766
6	gossypol	0.735
7	lanatoside C	0.733
8*	digitoxigenin	0.687
9*	valinomycin	0.680
10	8-azaguanine	0.671

Figure 3. PluriSIn #1 Induces ER Stress, Protein Synthesis Attenuation, and Apoptosis in hPSCs

(A) The chemical structure of the 15 identified PluriSIns. Phenylhydrazine, a common moiety shared by nine of these 15 compounds, is marked in red.

(B) Gene expression-based unsupervised hierarchical clustering of undifferentiated ESCs and eight day-differentiated endodermal progenitor cells, treated with PluriSIn #1, PluriSIn #6, or without treatment (DMSO control). The heat map presents all differentially expressed genes (>2-fold) between control and treatment conditions.

(C) Gene expression fold change of selected genes related to apoptosis, in undifferentiated ESCs and in eight day-differentiated endodermal progenitor cells, 12 hr after their exposure to PluriSIn #1 or PluriSIn #6 (20 μM).

(D) Representative FACS analysis of undifferentiated cells under DMSO control conditions (top) or exposed to PluriSIn #1 (20 μM, bottom) for 16 hr, confirming that exposure to PluriSIn #1 induces apoptosis in the cells.

(E) Quantification of the increase in early and late apoptotic cells. Data are presented as mean ± SD.

(F) Immunoblots with an antibody against caspase-3, showing elevated activation in ESCs treated with PluriSIn #1 (20 μM). β-catenin is presented as loading control; dithiothreitol (DTT) is presented as positive control.

(G) Quantification of cell viability after 24 hr exposure of human ESCs to PluriSIn #1 (20 μM) in the presence or absence of the pancaspase inhibitor Z-VAD-FMK. Data are presented as mean ± SD.

(H) Gene expression fold change of selected genes related to ER stress, in undifferentiated ESCs and in eight day-differentiated endodermal progenitor cells, 12 hr after their exposure to PluriSIn #1 or PluriSIn #6 (20 μM). Gene expression change conferred by the general ER stress inducer DTT is presented as positive control.

(I) Top: quantitative PCR analysis of the spliced variant of XBP1 (sXBP1), a hallmark of the unfolded protein response, in undifferentiated ESCs and in differentiated fibroblasts. RPB1 was used as endogenous control. Data are presented as mean ± SD. Bottom: immunoblots with an antibody against phosphorylated eIF2α (phospho-eIF2α), showing elevated phosphorylation level in ESCs treated with PluriSIn #1 but not in differentiated cells treated with the compound. α-tubulin is presented as loading control; in both experiments, DTT (1 mM) is presented as positive control.

(J) The list of ten compounds ranked by the connectivity map as most similar to PluriSIn #1, in terms of the global gene expression changes they confer. The mean connectivity score represents the degree of similarity (on a scale of −1 to 1). Protein synthesis inhibitors are denoted with red asterisks and are overrepresented in this list (65-fold enrichment, $p < 0.0001$). Black asterisks denote compounds that are not defined in cmap as protein synthesis inhibitors but are known to attenuate protein translation.

(K) Relative incorporation of S^{35}-labeled methionine in ESCs and in differentiated fibroblasts, 12 hr after their exposure to PluriSIn #1 (20 μM) or to DMSO control conditions. Data are presented as CPMA reads normalized to the total protein quantity. These results indicate that PluriSIn #1 induces protein synthesis attenuation in hPSCs but not in differentiated cells. The general protein synthesis inhibitor cycloheximide (10 μM) is presented as positive control. Data are presented as mean ± SD. See also Figure S5.

conducted using DAVID functional annotation tool (Huang et al., 2009) and revealed enrichment for apoptosis (2.7-fold enrichment, p = 0.007 after Benjamini correction). We therefore performed an Annexin V apoptosis assay after 16 hr and 18 hr exposure of undifferentiated cultures to PluriSIn #1, revealing a gradual and significant increase in the percentage of apoptotic cells in culture (Figures 3D, 3E, and S5A). Moreover, immunoblotting with a specific antibody against caspase-3 demonstrated the activation of this hallmark executioner of apoptosis after PluriSIn #1 treatment (Figure 3F). Lastly, exposure of hPSCs to PluriSIn #1 in the presence of the pancaspase inhibitor Z-VAD-FMK significantly suppressed PluriSIn #1-induced cell death (Figure 3G). Together, these results confirm that apoptosis is the central cell death mechanism activated by PluriSIn #1.

Among the most deregulated genes, we also detected multiple genes related to endoplasmic reticulum (ER) stress and unfolded protein response (UPR) (Figure 3H). The most upregulated gene after PluriSIn treatment was *CHOP* (also known as DDIT3), a hallmark of UPR (9-fold increase, p = 0.01). To further examine UPR in our system, we studied two of its hallmarks: XBP1 mRNA splicing and phosphorylation of eIF2α (Hetz, 2012). Quantitative PCR revealed ~3.5-fold increase in the expression of the spliced isoform sXBP1 after exposure of hPSCs to PluriSIn #1 (p = 0.007, Figure 3I, top); immunoblotting with a specific antibody against phosphorylated eIF2α showed a marked increase of phosporylation (Figure 3I, bottom). Thus, these assays confirmed that PluriSIn #1 leads to ER stress in hPSCs.

We then applied the gene expression data to the connectivity map (cmap), a database of genome-wide transcriptional expression data from cultured human cells treated with bioactive small molecules (Lamb et al., 2006). Cmap was developed to facilitate the discovery of pathways perturbed by small molecules of unknown activity, based on the common gene expression changes that similar small molecules confer (Lamb et al., 2006). We thus queried this database with the deregulated gene lists, i.e., the lists of genes that were at least 2-fold upregulated or downregulated after a 12 hr treatment with PluriSIn #1. ER stress does not appear as a distinct category in the cmap database (Iorio et al., 2010). However, this analysis indicated that PluriSIns are most similar to protein synthesis inhibitors (PSIs), as PSIs were ranked highest in the list, with very high connectivity scores (Figure 3J). Only four compounds are classified as bona fide PSIs in the cmap database (Iorio et al., 2010), and all of them appeared among the ten most similar compounds to PluriSIn #1 (65-fold enrichment, p < 0.0001). As ER stress can indeed lead to translational attenuation, we tested directly the effect of PluriSIn #1 treatment on protein synthesis. Using a pulse-chase radioactive labeling assay, we measured the incorporation of 35S-Met into the cells in the presence or absence of PluriSIn #1. The results confirmed that PluriSIn #1 induces ~30% decrease in protein synthesis in hPSCs (p = 0.005, Figure 3K). Importantly, no apoptosis, ER stress, or translation attenuation could be detected in differentiated cells exposed to PluriSIn #1 (Figures 3C, 3H, 3I, and 3K). Moreover, no significant gene expression change was induced in cells exposed to PluriSIn #1 after merely 8 days of differentiation (Figure 3B), showing that the transcriptional landscape of differentiated cells is not hindered by exposure to this compound. Thus, we confirmed that upon exposure to PluriSIn #1, undifferentiated cells are selectively destroyed, whereas differentiated cells remain intact.

Inhibition of SCD1 Underlies the Cellular Response to PluriSIn #1

All of the 15 PluriSIns had been previously screened at Roche and had never come up as cytotoxic. One of these nonrelated screens, performed in the context of drug discovery of metabolic disorders, was a biochemical screen aimed to identify inhibitors of stearoyl-coA desaturase (SCD1), an ER-membrane protein that is the key enzyme in the biosynthesis of monounsaturated fatty acids (MUFAs). The compounds in that screen were tested in a radiometric assay that monitors the formation of 3H-water from the SCD1-catalyzed desaturation of 3H (9,10) stearoyl-CoA to oleoyl-CoA, using murine liver microsomes as the source of the enzyme (Miyazaki et al., 2000). When we searched Roche databases for the 15 identified PluriSIns, we noticed that three of them, including PluriSIn #1, had come up as "hits" in that direct SCD1 inhibition assay. Inhibition of SCD1 was recently shown to induce ER stress and UPR in some human cancer cell lines, leading to apoptosis of these cells, and was thus suggested to be a potential target for cancer therapy (Hess et al., 2010; Mason et al., 2012; Minville-Walz et al., 2010; Roongta et al., 2011). SCD1 is expressed in hPSCs (Assou et al., 2007), but its role in these cells has not been described to date. The similarity between the hPSC response to PluriSIn #1 and the response of some cancer cell lines to SCD1 inhibitors led us to explore whether SCD1 inhibition may underlie the cellular response of hPSCs to PluriSIn #1.

We therefore compared the gene expression changes that we observed in hPSCs after their exposure to PluriSIn #1, with those previously detected in a human cancer cell line (H1299) after the pharmacological inhibition of SCD1 by its specific inhibitor A939572 (Roongta et al., 2011). We observed an intriguing similarity between the expression changes: 12 of the 18 genes that exhibited significant expression changes in the study of Roongta et al. (p < 0.05, >2-fold change), many of which related to the ER stress pathway, were also significantly deregulated in our cells (Figure 4A). In order to directly examine whether PluriSIn #1 inhibits SCD1 activity in pluripotent cells, we performed a pulse-chase labeling assay. Human ESCs were treated with PluriSIn #1 for 12 hr and were then labeled with [1-^{14}C] stearic acid, the substrate of SCD1, in the presence of the compound. After ~4 hr of incubation, lipids were purified from the cells and separated by TLC. The enzymatic activity was then evaluated by direct measurement of the radioactive intensities of SCD1 substrate and product, [1-^{14}C] oleic acid. The results showed an ~65% decrease in SCD1 activity after the exposure of hPSCs to PluriSIn #1, in comparison to its activity in DMSO-treated control cells ($p = 2.1 \times 10^{-6}$, Figure 4B). These results indicate that PluriSIn #1 indeed inhibits SCD1 activity in hPSCs.

To validate that SCD1 inhibition can really lead to cell death in hPSCs, we abolished its activity both pharmacologically and genetically: treatment of human ESCs either with structurally distinct specific SCD1 inhibitors (A939572 and CAY10566) or with specific siRNAs against *SCD1* resulted in massive cell death (>80% decrease in cell viability on exposure to A939572

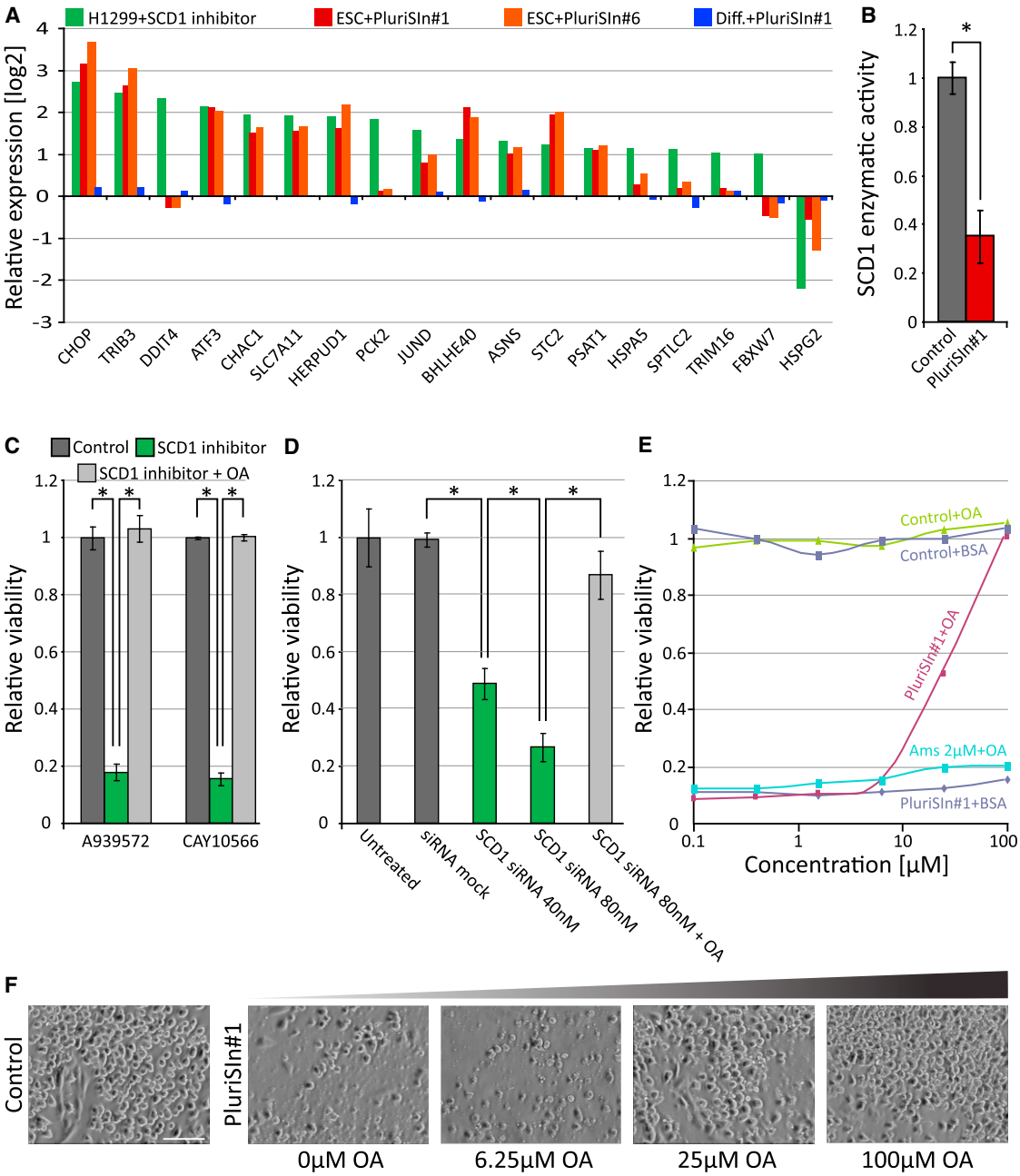

Figure 4. Inhibition of SCD1 Activity Underlies the Cellular Response of hPSCs to PluriSIn #1

(A) Gene expression fold change of the 18 genes previously identified to be upregulated or downregulated upon treatment of cancer cells (H1299) with A939572, a specific inhibitor of SCD1 (Roongta et al., 2011). A similarity was found between the effect of SCD1 inhibitor on cancer cells to that of PluriSIn #1 on hPSCs but not on eight day-differentiated cells.

(B) Direct measurement of SCD1 enzymatic activity in undifferentiated hPSCs treated with control DMSO or with PluriSIn #1 (20 μM), confirming that PluriSIn #1 inhibits SCD1 activity in hPSCs. Data are presented as mean ± SD.

(C) Quantification of the relative number of viable human ESCs under DMSO control conditions and after treatment with the SCD1 inhibitors A939572 or CAY10566 (75 nM), in the presence or absence of oleic acid (100 μM). Data are presented as mean ± SD.

(D) Quantification of the relative number of viable human ESCs transfected with mock-siRNA or with siRNA against *SCD1*. Data are presented as mean ± SD.

(E) Quantification of the relative number of viable human ESCs under DMSO control conditions or after treatment with PluriSIn #1 (20 μM), in the presence or absence of oleic acid conjugated to BSA. Oleic acid rescued the PluriSIn #1-induced cell death in a dose-dependent manner (red), while not affecting the growth of control cells (green) and not rescuing the cell death induced by amsacrine hydrochloride (light blue). Note that BSA alone did not rescue PluriSIn #1-induced cell death (light purple) and did not affect the growth of control cells (dark purple).

(F) Representative images of hPSCs treated with PluriSIn #1 (20 μM) and with increasing concentrations of oleic acid. An image of the cells under DMSO control conditions is presented for reference. Scale bar represents 100 μm. See also Figure S5.

and CAY10566 and ~70% decrease after knockdown; $p = 6 \times 10^{-6}$, 2×10^{-5}, and 2×10^{-3}, respectively), confirming that hPSCs depend on MUFA synthesis for their survival (Figures 4C and 4D). Remarkably, exogenous supplementation of oleic acid, the direct product of SCD1 activity, rescued the cell death induced by these pharmacologic and genetic perturbations (Figures 4C and 4D; $p = 3 \times 10^{-4}$, 1×10^{-4}, and 6×10^{-3}, respectively).

We reasoned that if PluriSIn-induced apoptosis in hPSCs occurred due to interference with the enzymatic activity of SCD1, then this cell death could also be rescued by exogenous supplementation of oleic acid. We therefore exposed the cells to PluriSIn #1 in the presence of increasing concentrations of oleic acid. Remarkably, medium supplementation with oleic acid led to a concentration-dependent suppression of cell death, with full rescue observed in the presence of high concentrations of this fatty acid (Figures 4E and 4F). Collectively, these data reveal that the survival of hPSCs depends on the normal activity of SCD1 and that hPSCs are highly sensitive to perturbations in the MUFA biosynthesis pathway. Similarly to some cancer cell lines, inhibition of SCD1 activity in hPSCs leads to MUFA depletion, which induces ER stress and UPR followed by translational attenuation, and ultimately results in apoptosis of the cells (see Discussion section). To further confirm that SCD1 inhibition underlies the cellular perturbations observed after the exposure of hPSCs to PluriSIn #1, we examined whether the SCD1 inhibitor A939572 would recapitulate these cellular responses. We found that, similarly to PluriSIn #1, exposure of hPSCs to A939572 results in ER stress, protein synthesis inhibition, and apoptosis (Figures S5A–S5C).

The finding that nine of 15 PluriSIns share a common moiety, phenylhydrazine, and seven of them are N-acyl phenylhydrazine derivatives suggested that these compounds might work through the same molecular target and/or mechanism of action. We thus examined whether four other PluriSIns also work through the inhibition of SCD1: two PluriSIns with N-acyl phenylhydrazine in their structure (PluriSIn #5 and PluriSIn #6) and two PluriSIns that do not contain this phenylhydrazine (PluriSIn #2 and PluriSIn #3). HPSCs were exposed to each of these PluriSIns for 24 hr, at the presence or absence of oleic acid, and cell viability was then quantified. Remarkably, oleate prevented PluriSIn #5- and PluriSIn #6-induced hPSC death but had no effect on the cell death induced by PluriSIn #2 or PluriSIn #3 (Figure S5D). These results imply that some, but not all, of the PluriSIns work through the inhibition of SCD1, and that the common moiety may indeed be related to this effect. Supporting this hypothesis, PluriSIn #6 conferred gene expression alterations that were highly similar to those conferred by PluriSIn #1 (Figure 3B) and that predicted SCD1 inhibition (Figure 4A), UPR (Figure 3H), PSI (Figure S5E), and apoptosis (Figure 3C). Further research is warranted to elucidate the mechanism of action and the molecular targets of other PluriSIns.

PluriSIn #1 Compromises Mouse Embryonic Development

Mouse PSCs (mPSCs) are widely used in pluripotency-related research, and generating pure cultures of mPSC-differentiated cells is therefore of great importance. We were thus interested to determine whether mPSCs are also sensitive to PluriSIns. R1 Oct4-GFP mouse ESCs were plated in 96-well plates and exposed to PluriSIns at 20 μM concentration, and the viability of the cells was then assessed at 24 hr, 48 hr, and 72 hr, using luminescent viability assay and fluorescence microscopy imaging. The four examined PluriSIns induced massive cell death in mPSCs, indicating that PluriSIn sensitivity is shared by mouse and human PSCs (Figures 5A and 5B). It is worth noting, however, that inhibition of mPSCs by PluriSIns was not as efficient as that of hPSCs and required a longer exposure to the compounds (Figures 5A and 5B).

We next took advantage of the mouse system to examine whether PluriSIn #1 is cytotoxic to the inner cell mass cells (ICMCs), from which ESCs are derived. We figured that if SCD1 activity was crucial to pluripotent cells in vivo, then PluriSIn #1 would be cytotoxic to the ICMCs and would thus compromise normal embryonic development. We cultured mouse embryos from the two-cell stage, exposed them to PluriSIn #1 at the morula stage, and followed their development. All of the control embryos (18/18) developed into blastocysts with large and distinct (grade A/B) ICMCs (Figures 5C and 5D). In contrast, only ~40% of the embryos exposed to PluriSIn #1 developed into high-quality blastocysts (7/17), whereas the rest of these embryos developed into blastocysts with no distinguished ICMCs (grade C, 6/17) or were "stuck" at the morula stage (4/17) (Figures 5C and 5D). This marked difference in the embryonic fate after exposure to the compound is highly significant ($p = 0.0001$) and indicates that PluriSIn #1 is indeed cytotoxic to ICMCs and precludes normal development of the blastocyst. We next examined whether oleic acid supplementation would rescue blastocyst formation; most embryos exposed to PluriSIn #1 in the presence of oleic acid developed into high-quality blastocysts (5/7) (Figures S6A and 5D), a much greater proportion than in the embryos exposed to PluriSIn #1 alone (71% versus 41%, respectively). Finally, we examined whether blastocyst formation would also be hindered by the SCD1 inhibitor A939572; indeed, only half of the embryos exposed to this compound developed into high-grade blastocysts (5/9, $p = 0.007$), and this proportion increased after oleic acid supplementation (5/7) (Figures S6A and S6B). These results suggest that the dependence of PSCs on SCD1 is inherent to the pluripotent state, both in vitro and in vivo.

PluriSIn #1 Can Prevent Teratoma Formation

As the ultimate goal of selective hPSC inhibitors is to prevent teratoma formation by efficiently removing residual undifferentiated cells from culture, we next turned to demonstrate the usefulness of PluriSIn application for this aim, using in vitro and in vivo assays. We tested the compounds in various culture conditions and exposure durations and found that PluriSIns were more potent in smaller (384- or 96-well) plates than in larger (6-well or 10 cm) plates, and in low cell densities than in high cell densities, probably due to a protective effect conferred by large colonies (Figure S7A). For the complete elimination of undifferentiated cells cultured in 6-well plates, 48 hr exposure of the cells to PluriSIn #1 at 20 μM was required (Figure S7B). Of note, PluriSIns were also more potent when cells were cultured on matrigel-coated plates without feeder cells, using mTeSR1-defined medium; hPSCs cultured on MEFs with regular ESC medium were less sensitive to PluriSIns, possibly due to

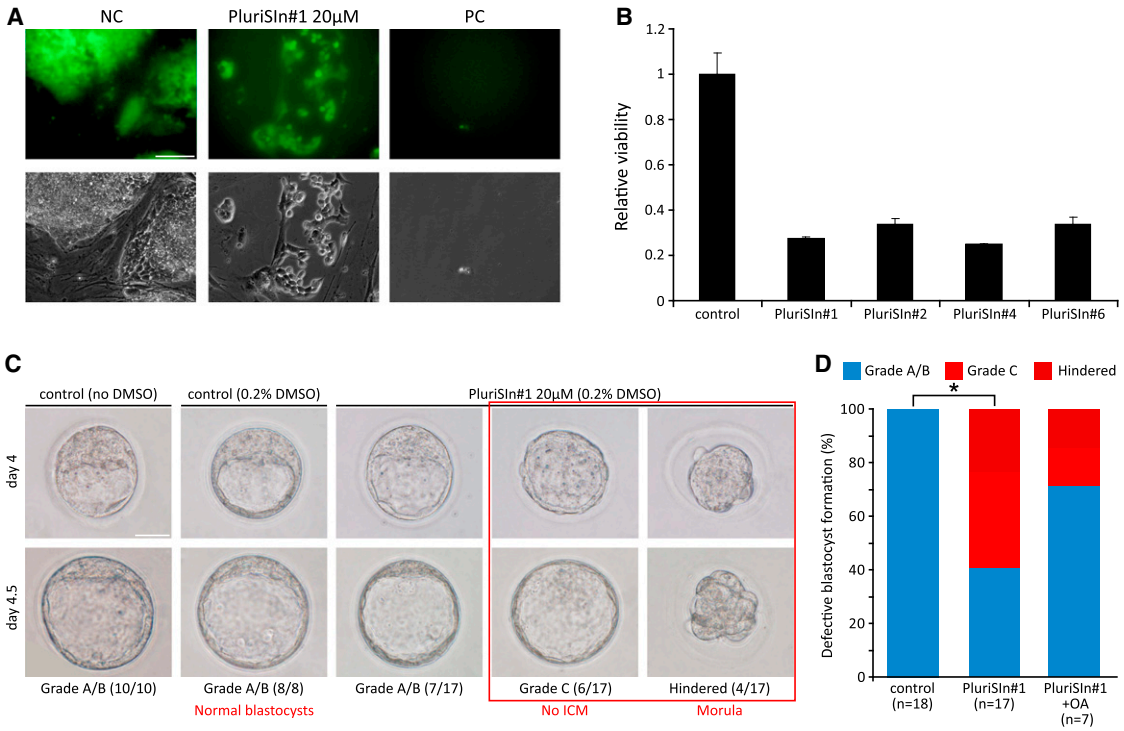

Figure 5. PluriSIns Inhibit Mouse Pluripotent Stem Cells and Hinder Mouse Embryonic Development

(A) Fluorescence microscopy imaging of undifferentiated R1 Oct4-GFP mouse ESCs. NC, negative control, 0.5% DMSO; PC, positive control, amsacrine hydrochloride at 5 μM. Scale bar represents 100 μm.

(B) Quantification of the relative number of viable mouse ESCs under DMSO control conditions or after treatment with various PluriSIns (20 μM) for 72 hr. Data are presented as mean ± SD.

(C) Representative images of mouse embryos developed in vitro from the two-cell stage (1.5 dpc) to the mature blastocyst stage (4.5 dpc). At the morula stage (3.5 dpc), embryos were exposed for 24 hr to PluriSIn #1 (20 μM) or to control conditions (0.2% DMSO or without DMSO at all). All 18 embryos grown under control conditions developed into mature blastocysts with distinct inner cell mass, whereas only seven of 17 embryos grown in the presence of PluriSIn #1 developed into such blastocysts ($p = 0.0001$); ICM, inner cell mass. Note that embryos without inner cell mass, and embryos stuck at the morula stage, were observed upon PluriSIn #1 treatment. Scale bar represents 100 μm.

(D) A stacked column graph presenting the percentage of grade A/B, grade C, and hindered blastocysts, after the exposure of mouse embryos to control conditions, to PluriSIn #1 (20 μM) alone, or to PluriSIn #1 together with oleic acid (100 μM). See also Figure S6.

the different media compositions or due to a protective effect of the MEFs (Figure S7C).

We next set out to determine the number of residual undifferentiated cells that remain in culture after PluriSIn #1 application in vitro, and whether these remaining cells would be tumorigenic in vivo. Fluorescence-activated cell sorting (FACS) analysis of mixed cell populations cultured in 6-well plates and exposed to PluriSIn #1 for 48 hr suggested that over 99% of the pluripotent cells are eliminated from culture, based on their staining to the pluripotent marker TRA-1-60 (Figure 6A). Fluorescence microscopy imaging of CSES-SO2/3 cells after treatment confirmed that almost all OCT4-expressing cells were eliminated (Figure 6B). We then mixed hPSCs with differentiated cells (a customary methodology for teratoma formation analysis; Hentze et al., 2009; Tang et al., 2011) and examined the ability of PluriSIn #1 to prevent teratomas. hPSCs were differentiated for 10 days, mixed with undifferentiated cells (1:1), exposed to PluriSIn #1 for 48 hr, and then injected subcutaneously into immune-compromised mice. We used the highly immune-deficient strain NOD-SCID IL2Rγ−/− mice, which was previously shown to be especially susceptible to develop human-derived tumors (Quintana et al., 2008). Each mouse was injected with PluriSIn #1-treated cells into one side of its body and DMSO-treated control cells into the other side. Importantly, the same total number of cells (~1×10^6) was injected into both sides. Mice were sacrificed after 6 weeks, and teratoma formation was assessed. As expected, all the injected mice developed teratomas only in the side injected with control hPSCs (Figures 6C, 6D, S7D, and S7E), whereas no teratomas were generated in any of the mice transplanted with PluriSIn #1-treated hPSCs (Figures 6E, S7D, and S7E). Treatment of the cells with the SCD1 inhibitor A939572 recapitulated the preventive effect of PluriSIn #1 (Figure S7F). To verify that PluriSIn #1-treated hPSCs do not generate teratomas even after prolonged time in vivo, the cells were injected into four mice subcutaneously, and teratoma formation was monitored every week for 16 weeks. No teratomas were generated in any of these mice throughout the entire time course of the experiment. We conclude that PluriSIn #1 can efficiently remove tumorigenic undifferentiated cells from cultures of hPSC-derived cells.

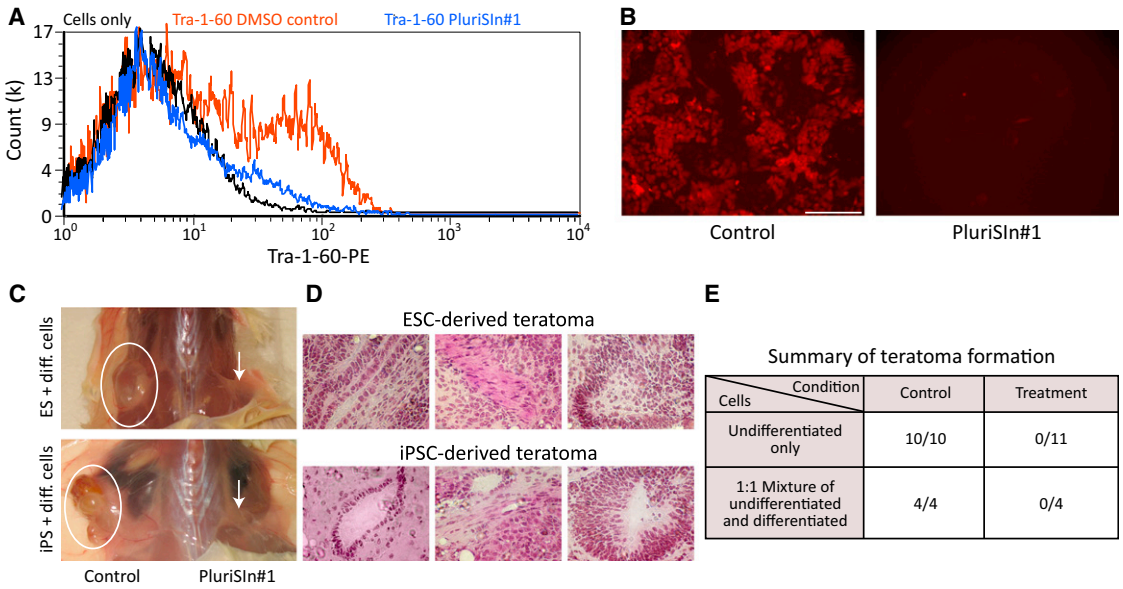

Cells \ Condition	Control	Treatment
Undifferentiated only	10/10	0/11
1:1 Mixture of undifferentiated and differentiated	4/4	0/4

Figure 6. PluriSIn #1 Prevents Teratoma Formation from Undifferentiated hPSCs

(A) Human ESCs were differentiated in culture for 10 days and were then mixed with undifferentiated ESCs in 6-well plates and exposed to PluriSIn #1 or to DMSO control conditions for 48 hr. Cells were stained with an antibody against TRA-1-60, and the fraction of remaining undifferentiated cells in culture was examined by FACS analysis. Whereas a large fraction of TRA-1-60-positive cells existed in the control culture (red), the PluriSIn #1-treated culture (blue) was comprised of differentiated cells only (with less than 1% TRA-1-60-positive cells).

(B) Fluorescence microscopy imaging of CSES-SO2/3 cells grown in 6-well plates, after 48 hr exposure to DMSO control conditions or to PluriSIn #1 (20 μM). OCT4-positive cells were not detected in culture after PluriSIn #1 treatment (red fluorescence). Scale bars represent 200 μm.

(C) Human ESCs and iPSCs were spontaneously differentiated in culture for 10 days and were then mixed 1:1 with undifferentiated cells. After 48 hr exposure to PluriSIn #1, cells were harvested and injected subcutaneously into NOD-SCID IL2Rγ−/−. Each mouse was injected with PluriSIn #1-treated cells into one side of its back and control-treated cells into the other side. The same total number of cells (approximately one million) was injected into both sides. Six weeks later, mice were sacrificed. Only the control cells generated teratomas (encircled), whereas the injected PluriSIn #1-treated cells did not (arrows indicate the locations of their injections).

(D) Histology of ESC- and iPSC-derived teratomas stained with hematoxylin and eosin. From left to right: representative gut epithelium, skeletal muscle, and neural rosette structures are presented. Scale bar represents 100 μm.

(E) A summary of teratoma formation experiments, showing that all of the control cells—but none of the cells treated with PluriSIn #1—formed teratomas. See also Figure S7.

DISCUSSION

We performed a high-throughput screen of 52,448 small molecules and identified 696 compounds that efficiently and rapidly eliminate human ESCs and iPSCs in a concentration-dependent manner. We then counter screened these compounds against nine cell types of all developmental stages and of all germ layers and identified small molecules that selectively eliminated hPSCs, without reducing the viability of any other cell type, including other stem and progenitor cells. We thus termed these compounds pluripotent-specific inhibitors (PluriSIns). In order to identify the molecular target and the pathway perturbed by these molecules, we first took a toxicogenomic approach and explored the gene expression changes conferred by exposure of hPSCs to selected PluriSIns. Gene expression patterns of hPSCs after 12 hr exposure to PluriSIn #1 suggested that it may lead to ER stress, UPR, PSI, and apoptosis. Direct biochemical assays revealed that PluriSIn #1 inhibits SCD1, the key enzyme in the generation of MUFA, and that this inhibition in hPSCs indeed results in ER stress, UPR, PSI, and finally apoptosis. Supplementation of the medium with oleic acid, the product of SCD1 activity, completely rescued the PluriSIn #1-induced cell death, indicating that SCD1 inhibition is the direct cause of death.

These data reveal a previously uncharacterized dependence of hPSCs on SCD1 activity, related to that seen previously in human cancer cell lines. This dependence is evolutionarily conserved, as PluriSIn #1 was cytotoxic to mPSCs as well. Importantly, PluriSIn #1 was also cytotoxic to the ICMCs of developing mouse blastocysts, suggesting that the dependence of PSCs on SCD1 is inherent to the pluripotent state. Interestingly, *Scd1* knockout is not embryonic lethal in mice (Miyazaki et al., 2000), probably due to its functional redundancy with three other mouse Scd isoforms (Scd2, Scd3, and Scd4) that share about 85% amino acid identity with the protein product of *Scd1* (Ntambi et al., 2004) and that do not exist in humans.

Finally, we demonstrated the usefulness of PluriSIns for the complete removal of tumorigenic hPSCs from culture and prevention of teratoma formation. The teratoma experiments were performed by mixing undifferentiated cells with their differentiated progeny, rather than by transplanting differentiated cultures per se. This approach is well accepted in the field (Hentze et al., 2009; Tang et al., 2011), as the baseline

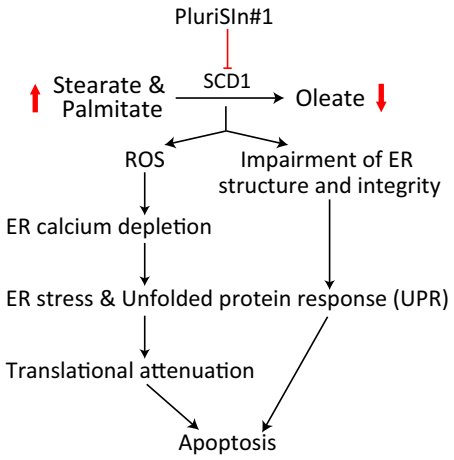

Figure 7. A Model of PluriSIn #1 Mechanism of Action

A model of PluriSIn #1 mechanism of action, based on all presented data. PluriSIn #1 inhibits SCD1 activity in hPSCs, thereby altering the balance between its substrates and its products, leading to the accumulation of palmitate and stearate and to the deprivation of oleate. This inhibition selectively leads to ER stress, unfolded protein response, and translational attenuation in hPSCs, which finally result in apoptosis. See the Discussion section for elaborated explanation of the model.

incidence of teratoma formation upon transplantation of differentiated cultures is low to begin with (Miura et al., 2009; Roy et al., 2006; Xie et al., 2007). The results from these experiments show that PluriSIns can be used to drastically reduce the risk of tumor formation after injection of hPSC-derived cells into patients and can thus considerably improve the safety of hPSC-based treatments.

Lipids were previously reported to regulate the self-renewal of human ESCs (Garcia-Gonzalo and Izpisúa Belmonte, 2008), but no specific lipid was determined to be essential for the survival of these cells. Here we found that the biosynthesis of the MUFA oleate by the enzyme SCD1 is a vital process in hPSCs. As the expression level of SCD1 in hPSCs is comparable with that of other cell types, such as fibroblasts and neural cells, and is lower than that in hepatocytes (Assou et al., 2007), the specific cytotoxicity of PluriSIn #1 toward hPSCs cannot be explained by a uniquely high expression of this protein in hPSCs. Importantly, although media composition can influence the sensitivity of hPSCs to PluriSIn #1 (as is evident by the oleate supplementation experiments), this cannot explain the selective cytotoxic effect either: the defined medium mTeSR1 contains oleate at a concentration of 10 μM (Ludwig et al., 2006), whereas the serum-free Dulbecco's modified Eagle's medium that we used for endodermal differentiation did not contain any oleic acid; nonetheless, hPSCs grown with mTeSR are highly sensitive to PluriSIn #1, while eight day-differentiated cells are completely resistant to it. Moreover, when we cultured several PluriSIn #1-resistant cell types in human ESC medium and exposed them to PluriSIn #1, the compound still did not have any cytotoxic effect on these cells (Figures S4C and S4D), ruling out the medium as an important factor in the differential PluriSIn #1-induced lethality.

Previous studies in various cell types have shown that accumulation of saturated fatty acids, SCD1 substrates, and depletion of MUFA, SCD1 product, can induce ER stress and UPR by several mechanisms: generation of reactive oxygen species (ROS), which leads to ER calcium depletion (Borradaile et al., 2006a); alteration of the ER membrane composition, which results in a dramatic impairment of its structure and integrity (Borradaile et al., 2006b); and impairment of the ER-to-Golgi trafficking, which results in the build-up of proteins in the ER (Preston et al., 2009). Oleic acid, the product of SCD1 activity, was shown to compete with the saturated fatty acids, block the abnormal lipid distribution, and attenuate ER stress (Hapala et al., 2011; Peng et al., 2011). Our findings reveal that hPSCs require oleate for their survival and are thus highly sensitive to SCD1 inhibition, which activates a cascade of events that culminates in the death of these cells (Figure 7). Importantly, differentiated cell types are much less sensitive to SCD1 inhibition, and this difference seems to underlie the selective cell death conferred by SCD1 inhibitors. According to our proposed model, the selectivity of PluriSIn #1 is determined already early on in the cascade of events (i.e., by the selective response to SCD1 inhibition). Consistent with this model, general inducers of ER stress and PSI lead to hPSC death, but this effect is not selective and cannot be rescued by oleate (Figure S4E).

The high sensitivity of hPSCs to SCD1 inhibition may be, at least in part, due to their increased sensitivity to ER stress in general. The levels of hallmark UPR markers were shown to be high in hPSCs and decrease upon differentiation (Liu et al., 2012), suggesting that hPSCs experience ER stress under normal culture conditions. In line with previous reports, we found that hPSCs indeed express higher levels of the UPR hallmarks sXBP1 and peIF2α, when compared to differentiated cells (Figure 3I). Hence, a further increase in the already high ER stress levels in these cells may immediately induce their apoptosis. Of note, the activity of another metabolic enzyme, the mithochondrial threonine dehydrogenase, was previously shown to be essential for the survival of mPSCs (Alexander et al., 2011). As we show here that hPSCs are extremely sensitive to perturbation of MUFA biogenesis, it is tempting to speculate that the unique metabolic state of hPSCs may make them especially amenable to perturbations of metabolic processes.

PluriSIns are potent small molecules to selectively eliminate hPSCs. This chemical approach to ablate tumorigenic hPSCs from culture is superior to previously described methods as it is more rapid, efficient, and robust. It does not involve any genetic manipulation of the cells, which may affect genomic stability and undergo spontaneous reversion. It also does not require cell sorting and can thus be applied to complex differentiation protocols that do not allow for single-cell dissociation. As we demonstrate, PluriSIns can prevent teratoma formation by treatment of the cells prior to their transplantation. Hence, they should promote the safety of hPSC-based treatments and facilitate the safe transplantation of larger cell numbers. It will be interesting to examine whether PluriSIns might also be applied in vivo, both for the elimination of hPSC-derived tumors and against germ cell tumors. Future studies should also examine the compatibility of PluriSIns with specific clinically relevant differentiation protocols and determine the optimal concentrations and exposure durations for each individual case. The mechanistic understanding of the PluriSIn mode of action, i.e., the functionally unique role of SCD1 revealed in

hPSCs, should be helpful in optimizing culture conditions to support the most effective elimination of these cells. Lastly, the finding that this mechanism is also crucial during early mammalian development paves the way to future studies of the unique metabolism in preimplantation embryos.

EXPERIMENTAL PROCEDURES

Cell Culture

Human ESC lines H9, CSES2, and CSES2-SO2/3, iPSC line BJ-iPS28, neuroblastoma cell line Kelly, hepatocarcinoma cell line Huh-7, cervical carcinoma cell line HeLa, teratocarcinoma cell line NTERA-2, and immortalized BJ fibroblasts cell line were cultured using standard conditions. Human iPSC-derived cardiomyocytes were purchased from Cellular Dynamics International. Human ESC-derived hepatocytes were purchased from Cellartis. R1 Oct4-GFP mouse ESCs were cultured using standard conditions. See Supplemental Experimental Procedures for full culture and differentiation protocols.

Chemical Library Screening

The CellTiter-Glo luminescent cell viability assay (Promega) was implemented as an HTS assay for chemical library screen in a 384-well format. For primary screen, a 52,448 compound screening library assembled with Roche internal compounds was tested in a 384-well format. For confirmation screens, counter screens, and compound profiling screens, compounds that were defined as "hits" were obtained from Roche proprietary compound inventory. See Supplemental Experimental Procedures for full details of the screen.

Global Gene Expression Analysis

Total RNA was extracted and subjected to Human Genome U133A 2.0 microarray platform (Affymetrix). Arrays were normalized using MAS5 algorithm in the Affymetrix Expression Console. See Supplemental Experimental Procedures.

SCD1 Activity Measurement

SCD1 activity was directly measured by [1-^{14}C] Stearic Acid labeling, followed by quantification of free [1-^{14}C] Stearic Acid (substrate) and [1-^{14}C] Oleic Acid (formed product). All solvents and reagents were purchased from Sigma-Aldrich. Experiments were performed in triplicates. See Supplemental Experimental Procedures for full details of the assay.

SCD1 Inhibition and Oleic Acid Rescue Assay

SCD1 inhibition was performed either by commercial SCD1 inhibitors or by siRNA against human *SCD1*. For the rescue assay, cells were treated with PluriSIns in the presence or absence of oleate. See Supplemental Experimental Procedures.

In Vitro Embryonic Development Experiments

Two-cell embryos were collected by standard procedure, exposed to small molecules at the presence or absence of oleate, and analyzed at ~4 days post-coitum (dpc) and ~4.5 dpc. See Supplemental Experimental Procedures for a full description of the procedure.

Teratoma Formation and Analysis

Cells were injected subcutaneously to the back of NOD-SCID IL2R$\gamma^{-/-}$ mice (Jackson Laboratory). Six weeks after injection, mice were sacrificed, and the formation of tumors was examined. See Supplemental Experimental Procedures for full details.

ACCESSION NUMBERS

Microarray data have been deposited under Gene Expression Omnibus (GEO) accession number GSE37040.

SUPPLEMENTAL INFORMATION

Supplemental Information includes seven figures, two tables, and Supplemental Experimental Procedures and can be found with this article online at http://dx.doi.org/10.1016/j.stem.2012.11.015.

ACKNOWLEDGMENTS

The authors would like to thank Hong Ma and Adva Maimon for their assistance with tissue culture; Dr. Eric Chiao, Dr. Josh Babiarz, Dr. Jenny Cohen, and Sei Kameoka for their assistance with assay development; Sean Walker for his assistance with the liquid handler; Dr. Ann Hoffman for her assistance with microscopy imaging; Dr. Rachel Eiges for her assistance with the in vitro embryonic development assay and for critically reading the manuscript; Dr. Sonia Steiner-Mordoch and Professor Oded Meyuhas for their assistance with the protein synthesis inhibition assay; Dr. Simona Ceccarelli for her assistance with the chemical analysis of compounds; Tamar Shiloach for her assistance with apoptosis assays; Dr. Eran Meshorer for the mouse ESCs and for critically reading the manuscript; Oded Kopper for the CSES2-SO2/3 cells; Professor Batsheva Kerem, Dr. Kyle Kolaja, Dr. Jacques Mizrahi, and Dr. David Mark for fruitful discussions and helpful suggestions. N.B. is the Herbert Cohn Chair in Cancer Research. U.B.-D. is a Clore Fellow. This work was supported by a grant from Hoffmann La Roche-Yissum collaboration. Q.F.G., M.G., M.B., and G.G. are employees of the company. R.G. and P.A. are former employees of the company.

Received: July 8, 2012
Revised: October 22, 2012
Accepted: November 16, 2012
Published: January 10, 2013

REFERENCES

Alexander, P.B., Wang, J., and McKnight, S.L. (2011). Targeted killing of a mammalian cell based upon its specialized metabolic state. Proc. Natl. Acad. Sci. USA *108*, 15828–15833.

Assou, S., Le Carrour, T., Tondeur, S., Ström, S., Gabelle, A., Marty, S., Nadal, L., Pantesco, V., Réme, T., Hugnot, J.P., et al. (2007). A meta-analysis of human embryonic stem cells transcriptome integrated into a web-based expression atlas. Stem Cells *25*, 961–973.

Ben-David, U., and Benvenisty, N. (2011). The tumorigenicity of human embryonic and induced pluripotent stem cells. Nat. Rev. Cancer *11*, 268–277.

Blum, B., Bar-Nur, O., Golan-Lev, T., and Benvenisty, N. (2009). The anti-apoptotic gene survivin contributes to teratoma formation by human embryonic stem cells. Nat. Biotechnol. *27*, 281–287.

Borradaile, N.M., Buhman, K.K., Listenberger, L.L., Magee, C.J., Morimoto, E.T., Ory, D.S., and Schaffer, J.E. (2006a). A critical role for eukaryotic elongation factor 1A-1 in lipotoxic cell death. Mol. Biol. Cell *17*, 770–778.

Borradaile, N.M., Han, X., Harp, J.D., Gale, S.E., Ory, D.S., and Schaffer, J.E. (2006b). Disruption of endoplasmic reticulum structure and integrity in lipotoxic cell death. J. Lipid Res. *47*, 2726–2737.

Choo, A.B., Tan, H.L., Ang, S.N., Fong, W.J., Chin, A., Lo, J., Zheng, L., Hentze, H., Philp, R.J., Oh, S.K., and Yap, M. (2008). Selection against undifferentiated human embryonic stem cells by a cytotoxic antibody recognizing podocalyxin-like protein-1. Stem Cells *26*, 1454–1463.

Garcia-Gonzalo, F.R., and Izpisúa Belmonte, J.C. (2008). Albumin-associated lipids regulate human embryonic stem cell self-renewal. PLoS ONE *3*, e1384.

Germain, N.D., Hartman, N.W., Cai, C., Becker, S., Naegele, J.R., and Grabel, L.B. (2012). Teratocarcinoma formation in embryonic stem cell-derived neural progenitor hippocampal transplants. Cell Transplant. *21*, 1603–1611.

Hapala, I., Marza, E., and Ferreira, T. (2011). Is fat so bad? Modulation of endoplasmic reticulum stress by lipid droplet formation. Biol. Cell *103*, 271–285.

Hentze, H., Soong, P.L., Wang, S.T., Phillips, B.W., Putti, T.C., and Dunn, N.R. (2009). Teratoma formation by human embryonic stem cells: evaluation of essential parameters for future safety studies. Stem Cell Res. (Amst.) *2*, 198–210.

Hess, D., Chisholm, J.W., and Igal, R.A. (2010). Inhibition of stearoylCoA desaturase activity blocks cell cycle progression and induces programmed cell death in lung cancer cells. PLoS ONE *5*, e11394.

Hetz, C. (2012). The unfolded protein response: controlling cell fate decisions under ER stress and beyond. Nat. Rev. Mol. Cell Biol. *13*, 89–102.

Huang, W., Sherman, B.T., and Lempicki, R.A. (2009). Systematic and integrative analysis of large gene lists using DAVID bioinformatics resources. Nat. Protoc. *4*, 44–57.

Iorio, F., Bosotti, R., Scacheri, E., Belcastro, V., Mithbaokar, P., Ferriero, R., Murino, L., Tagliaferri, R., Brunetti-Pierri, N., Isacchi, A., and di Bernardo, D. (2010). Discovery of drug mode of action and drug repositioning from transcriptional responses. Proc. Natl. Acad. Sci. USA *107*, 14621–14626.

Kopper, O., and Benvenisty, N. (2012). Stepwise differentiation of human embryonic stem cells into early endoderm derivatives and their molecular characterization. Stem Cell Res. (Amst.) *8*, 335–345.

Lamb, J., Crawford, E.D., Peck, D., Modell, J.W., Blat, I.C., Wrobel, M.J., Lerner, J., Brunet, J.P., Subramanian, A., Ross, K.N., et al. (2006). The Connectivity Map: using gene-expression signatures to connect small molecules, genes, and disease. Science *313*, 1929–1935.

Lee, A.S., Tang, C., Cao, F., Xie, X., van der Bogt, K., Hwang, A., Connolly, A.J., Robbins, R.C., and Wu, J.C. (2009). Effects of cell number on teratoma formation by human embryonic stem cells. Cell Cycle *8*, 2608–2612.

Liu, L., Liu, C., Zhong, Y., Apostolou, A., and Fang, S. (2012). ER stress response during the differentiation of H9 cells induced by retinoic acid. Biochem. Biophys. Res. Commun. *417*, 738–743.

Ludwig, T.E., Bergendahl, V., Levenstein, M.E., Yu, J., Probasco, M.D., and Thomson, J.A. (2006). Feeder-independent culture of human embryonic stem cells. Nat. Methods *3*, 637–646.

Mason, P., Liang, B., Li, L., Fremgen, T., Murphy, E., Quinn, A., Madden, S.L., Biemann, H.P., Wang, B., Cohen, A., et al. (2012). SCD1 inhibition causes cancer cell death by depleting mono-unsaturated fatty acids. PLoS ONE *7*, e33823.

Menendez, S., Camus, S., Herreria, A., Paramonov, I., Morera, L.B., Collado, M., Pekarik, V., Maceda, I., Edel, M., Consiglio, A., et al. (2012). Increased dosage of tumor suppressors limits the tumorigenicity of iPS cells without affecting their pluripotency. Aging Cell *11*, 41–50.

Minville-Walz, M., Pierre, A.S., Pichon, L., Bellenger, S., Fèvre, C., Bellenger, J., Tessier, C., Narce, M., and Rialland, M. (2010). Inhibition of stearoyl-CoA desaturase 1 expression induces CHOP-dependent cell death in human cancer cells. PLoS ONE *5*, e14363.

Miura, K., Okada, Y., Aoi, T., Okada, A., Takahashi, K., Okita, K., Nakagawa, M., Koyanagi, M., Tanabe, K., Ohnuki, M., et al. (2009). Variation in the safety of induced pluripotent stem cell lines. Nat. Biotechnol. *27*, 743–745.

Miyazaki, M., Kim, Y.C., Gray-Keller, M.P., Attie, A.D., and Ntambi, J.M. (2000). The biosynthesis of hepatic cholesterol esters and triglycerides is impaired in mice with a disruption of the gene for stearoyl-CoA desaturase 1. J. Biol. Chem. *275*, 30132–30138.

Ntambi, J.M., Miyazaki, M., and Dobrzyn, A. (2004). Regulation of stearoyl-CoA desaturase expression. Lipids *39*, 1061–1065.

Peng, G., Li, L., Liu, Y., Pu, J., Zhang, S., Yu, J., Zhao, J., and Liu, P. (2011). Oleate blocks palmitate-induced abnormal lipid distribution, endoplasmic reticulum expansion and stress, and insulin resistance in skeletal muscle. Endocrinology *152*, 2206–2218.

Preston, A.M., Gurisik, E., Bartley, C., Laybutt, D.R., and Biden, T.J. (2009). Reduced endoplasmic reticulum (ER)-to-Golgi protein trafficking contributes to ER stress in lipotoxic mouse beta cells by promoting protein overload. Diabetologia *52*, 2369–2373.

Quintana, E., Shackleton, M., Sabel, M.S., Fullen, D.R., Johnson, T.M., and Morrison, S.J. (2008). Efficient tumour formation by single human melanoma cells. Nature *456*, 593–598.

Roongta, U.V., Pabalan, J.G., Wang, X., Ryseck, R.P., Fargnoli, J., Henley, B.J., Yang, W.P., Zhu, J., Madireddi, M.T., Lawrence, R.M., et al. (2011). Cancer cell dependence on unsaturated fatty acids implicates stearoyl-CoA desaturase as a target for cancer therapy. Mol. Cancer Res. *9*, 1551–1561.

Roy, N.S., Cleren, C., Singh, S.K., Yang, L., Beal, M.F., and Goldman, S.A. (2006). Functional engraftment of human ES cell-derived dopaminergic neurons enriched by coculture with telomerase-immortalized midbrain astrocytes. Nat. Med. *12*, 1259–1268.

Schuldiner, M., Itskovitz-Eldor, J., and Benvenisty, N. (2003). Selective ablation of human embryonic stem cells expressing a "suicide" gene. Stem Cells *21*, 257–265.

Tang, C., Lee, A.S., Volkmer, J.P., Sahoo, D., Nag, D., Mosley, A.R., Inlay, M.A., Ardehali, R., Chavez, S.L., Pera, R.R., et al. (2011). An antibody against SSEA-5 glycan on human pluripotent stem cells enables removal of teratoma-forming cells. Nat. Biotechnol. *29*, 829–834.

Wernig, M., Benninger, F., Schmandt, T., Rade, M., Tucker, K.L., Büssow, H., Beck, H., and Brüstle, O. (2004). Functional integration of embryonic stem cell-derived neurons in vivo. J. Neurosci. *24*, 5258–5268.

Xie, X., Cao, F., Sheikh, A.Y., Li, Z., Connolly, A.J., Pei, X., Li, R.K., Robbins, R.C., and Wu, J.C. (2007). Genetic modification of embryonic stem cells with VEGF enhances cell survival and improves cardiac function. Cloning Stem Cells *9*, 549–563.